THE ASTROPHYSICAL JOURNAL, 460:L45–L48, 1996 March 20

A CLUSTER OF CLASS 0 PROTOSTARS IN SERPENS: AN *IRAS* HIRES STUDY

ROBERT L. HURT AND MARY BARSONY
Physics Department, University of California, Riverside, CA 92521
Received 1995 November 7; accepted 1996 January 4

ABSTRACT

We present new 12, 25, 60, and 100 μm high-resolution–processed (HIRES-processed) *IRAS* images of the nearby Serpens star-forming cloud core at FWHM resolutions of ~30″–1′. We use HIRES-processed point-source models of the *IRAS* emission to derive new flux values and flux upper limits for all the protostellar candidates in the Serpens core. Our fluxes (and flux upper limits) determine the spectral energy distributions necessary to derive the dust temperature, circumstellar mass, bolometric luminosity, and evolutionary status of each protostellar candidate. Remarkably, we find all five sources studied by Hurt, Barsony, & Wootten, FIRS 1, SMM 4, S68N, SMM 3, and SMM 2, to share the defining characteristics of class 0 protostars, the short-lived (a few times 10^4 yr), earliest observable protostellar stage. We can also set an upper limit of 8 $L_\odot$ on the preoutburst bolometric luminosity of the recently discovered "FU Ori" source in this region.

Subject headings: circumstellar matter — infrared: ISM: continuum — ISM: jets and outflows — stars: pre–main-sequence — techniques: image processing

1. INTRODUCTION

The Serpens cloud core is a region of great interest for star formation studies because of the striking variety of young stellar objects and associated phenomena it harbors. Near-infrared (NIR) surveys have revealed the presence of an embedded young star cluster in this nearby cloud core (d = 310 pc; de Lara, Chavarria-K, & López-Molina 1991). The pioneering NIR single-aperture photometer survey of the central ~5′ × 10′ (0.45 pc × 0.90 pc) cloud area by Strom, Vrba, & Strom (1976) uncovered 20 sources, designated SVS 1–SVS 20. Subsequent higher resolution, higher sensitivity NIR array camera imaging of the central 6′ × 5′ core resulted in a catalog of at least 51 NIR cluster members out of 163 total identified sources, implying a stellar density exceeding 450 pc^{-3} (Eiroa & Casali 1989, 1992). One faint NIR source has in the last year brightened by 4.1 mag at 2.2 μm and has been provisionally identified as a new "FU Ori" object (Hodapp 1995).

Millimeter continuum maps of the central 6′ × 5′ Serpens core reveal at least six cold dust continuum peaks. Most lack NIR counterparts (Casali, Eiroa, & Duncan 1993), making them prime protostellar candidates. The most luminous source in this field, FIRS 1 (Harvey, Wilking, & Joy 1984), is the source of highly collimated, nonthermal, radio jets (Curiel et al. 1993) and drives a molecular outflow (Torrelles et al. 1992). A recent multitransition H_2CO study of the millimeter continuum peaks, FIRS 1, SMM 2, SMM 3, SMM 4, and S68N, confirms the presence of central heating sources and substantial masses of circumstellar gas in each of these objects, suggesting that they may all be among the youngest class of protostars known (Hurt, Barsony, & Wootten 1996).

The youngest (a few times 10^4 yr) protostellar sources have been dubbed "class 0," designating objects which have yet to accrete the bulk of their initial main-sequence mass from their infall envelopes (André, Ward-Thompson, & Barsony 1993; Barsony 1994). Observationally, the defining characteristics for class 0 protostars include a high ratio of millimeter/submillimeter to bolometric luminosity, the presence of molecular outflows, invisibility shortward of 10 μm, and spectral energy distributions (SEDs) resembling modified blackbodies with $T \leq 30$ K. Definitive characterization of a protostellar source requires knowledge of its spectral energy distribution, from which one may infer dust temperature, source luminosity, and circumstellar mass.

Since protostellar SEDs peak at ~100–200 μm, and since the Serpens core protostellar candidates are separated by as little as 20″, high-resolution far-infrared (FIR) data are required to produce SEDs for these sources. Previously published Kuiper Airborne Observatory (KAO) maps of 100 μm emission at 35″–45″ resolution (Harvey et al. 1984) and *IRAS* Chopped Photometric Channel (CPC) maps of 50 μm (88″ resolution) and 100 μm (100″ resolution) emission (Zhang, Laureijs, & Clark 1988) separate the Serpens core into just two components. In hopes of better distinguishing the separate contributions of the known millimeter continuum and NIR sources, we have utilized the high-resolution (HIRES) (Fowler & Aumann 1994) processing capability recently offered by the Infrared Processing and Analysis Center (IPAC)[1] to produce the highest possible resolution FIR maps of the Serpens core from the *IRAS* data set and to model it as a distribution of point sources. In § 2 we describe our HIRES processing in detail, and in § 3 we present our results.

2. DATA PROCESSING

We have used the HIRES image construction algorithm (implemented in the YORIC package) to produce new *IRAS* 12, 25, 60, and 100 μm images of the Serpens core using the all-sky survey data (Fig. 1). This program uses the maximum correlation method (MCM; see Aumann, Fowler, & Melnyk 1990) to iteratively *construct* resolution-enhanced images in the four *IRAS* wavelength bands, producing the smoothest flux distribution that is consistent with the survey data.

The *IRAS* survey data consist of the responses of 62 rectangular survey detectors to celestial sources, with flux measurements read out typically every 0.5 along the scan

[1] The Infrared Processing and Analysis Center (IPAC) is funded by NASA as part of the *Infrared Astronomical Satellite* (*IRAS*) extended mission under contract to the Jet Propulsion Laboratory (JPL).

direction. Detector orientations relative to a given source varied between subsequent tracks, resulting in highly nonuniform point-source response functions across even arcminute scales. Although the detector sizes significantly exceeded the *IRAS* telescope's diffraction limit, the high degree of oversampling at different detector orientations allows for significant image restoration. The MCM algorithm as applied to HIRES processing fundamentally differs from other common image restoration techniques that deconvolve a point-source response from an initially blurry image. Instead, the HIRES algorithm simulates in software the *IRAS* detector responses to the current input image (which is initially chosen to be a flat, positive flux distribution) and statistically compares them with the actual *IRAS* detector responses. Multiplicative correction factors are then calculated for each pixel and applied to the current image to produce the next image. The process is iterated a specified number of times, using each output image as the next input image. Ultimately, the output images converge to the flattest brightness distribution consistent with the actual *IRAS* detector responses, potentially reaching the diffraction limit of the telescope (Fowler & Aumann 1994).

To derive photometry results for the closely spaced Serpens core sources, we have pushed our HIRES processing beyond typical "default" processing of 20 iterations in all bands. Given the high brightness (i.e., high signal-to-noise ratio), the good, uniform detector coverages (80–90 detector "footprints" contributing to each pixel's flux), and the presence of interesting source structure on subarcminute scales, we were able to obtain substantial improvements in image resolution in our Serpens core maps. Our processing "recipe" included standard "laundering" (preprocessing that corrects for known systematic effects including cross-scan striping and cosmic-ray hits), baseline subtraction, and an applied flux bias to prevent clipping of negative noise. We used the default pixel size of 15″.

The vast improvements in HIRES image quality may be seen in Figure 1 (Plate L4). The top panels show single-iteration FRESCOs that do not resolve the core. Intermediate numbers of iterations are presented in the middle panels, demonstrating the improvements gained by going beyond default processing. In particular, the 60 and 100 μm maps converge toward structures seen at 12 and 25 μm, suggesting the maps have not been overprocessed to the point of manifesting spurious structures. Qualitatively, there is no clear demarcation to indicate when the "correct" number of iterations has been reached, such that one has produced the highest resolution image consistent with the detector responses, yet has not overprocessed the image by creating significant artifacts. Only slight "ringing" is found at negligible levels around these sources; ringing can be a significant HIRES artifact when point sources are sitting on high backgrounds (this is not the case for the Serpens core). Correction factor variance (CFV) maps may be used as a semiquantitative convergence diagnostic; for strong sources the correction factors should approach 1 as the variances in the correction factors approach zero (Fowler & Aumann 1994). For *IRAS* data sets with typical coverages, the CFV values typically reach 0.01–0.001 at strong, converged sources (Levine & Surace 1993). The stronger sources in the Serpens core had CFV values of 0.04–0.06 after 20 iterations in all bands, and values of ~0.01 after 50 iterations at 12 and 25 μm and after 150 iterations at 60 and 100 μm.

Effective resolutions were calculated by averaging Gaussian fits to a grid of test "spikes" across beam sample maps. The exact resolution at a given map location depends on detector coverages and the emission morphology. The approximate postprocessing "beam sizes" of our final HIRES images are significantly smaller than the detector sizes, although not quite diffraction limited: 25″ × 40″ at 12 and 25 μm, 35″ × 45″ at 60 μm, and 50″ × 60″ at 100 μm, all with standard deviations of ~20%.

Such improved resolutions are still insufficient to unambiguously resolve the Serpens core sources, so we have derived fluxes and flux upper limits from a point-source model of the emission. We obtained a HIRES-processed image of our model by specifying the positions of known NIR and millimeter sources in a beam sample map. The YORIC package simulates the *IRAS* detector responses to the specified point sources using the same detector coverages attained for the corresponding survey data. The point-source model data set is HIRES processed in parallel with the actual survey data using the same number of iterations. The resulting maps based on our model (hereafter "model" maps) are subject to the identical HIRES processing effects as the maps derived from the survey data (hereafter "survey" maps). The two sets may be compared directly to assess the validity of the point-source model.

The bottom row of Figure 1 demonstrates the good agreement between the "survey" (*contours*) and final "model" (*gray scale*) maps. Fluxes from aperture photometry of resolved clumps in the "model" and "survey" maps agree to better than 5%. For purposes of placing good upper limits on the flux contributions from confused individual protostellar sources, the "model" maps give us a distinct advantage over aperture photometry—flux is automatically conserved between the sources, and even if there are subtle artifacts or positional shifts resulting from our extensive HIRES processing, such systematic effects would be equally represented in both sets of maps.

Our final point-source "model" map is based on the 12 point sources listed in Table 1. With the exception of FIRS 1 at 12 and 25 μm, all of the sources are confused. Within each resolved clump, the total observed flux was distributed among the contributing sources, with the proportions adjusted to obtain maximum consistency between the morphologies in the "model" and "survey" maps. Sources not contributing obviously to the "survey" map morphologies at a given wavelength were omitted from the model and are listed as 3 σ upper limits in Table 1. We note that the sources S68N, IRS 53/SMM 5, and the newly discovered "FU Ori" object are too closely spaced to allow their relative proportions of flux to be meaningfully determined from the map morphology. Therefore, we simply divided the available *IRAS* HIRES flux found in the "survey" maps evenly among the three objects. We conservatively treat these sources as having flux upper limits of twice the tabulated values, while noting these limits do not imply unambiguous "detections."

Our point-source model is not a unique solution to the underlying brightness distribution of the Serpens core. There is some flexibility in how the fluxes can be distributed among the points without dramatically changing the "model" image morphology. The point-source "model" maps tend to exhibit more compact structure than the "survey" maps. This may indicate faster convergence (photometric noise, which would slow convergence, is not added to the simulated detector data set), but may also suggest that the Serpens core sources may be

PLATE L4

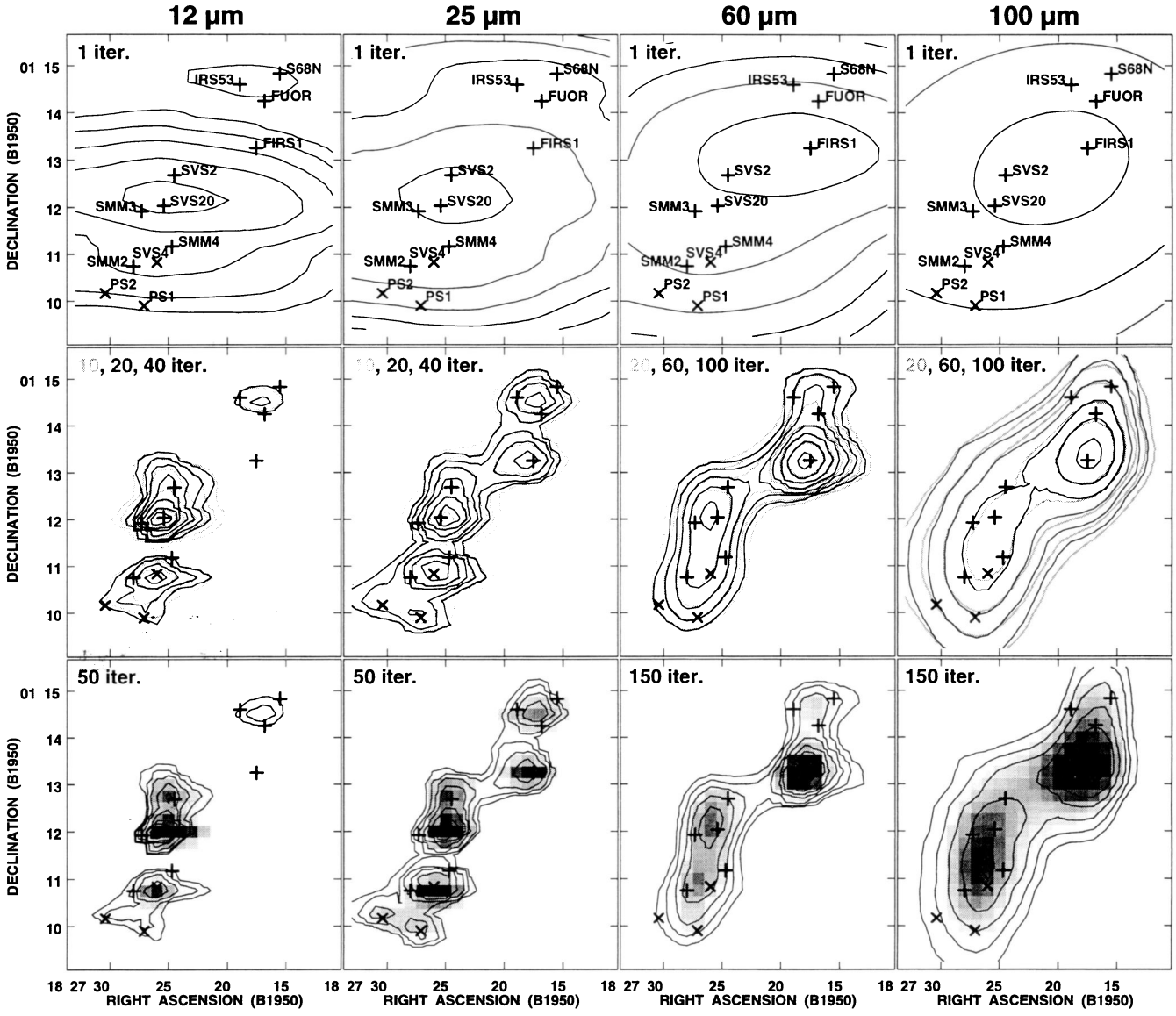

Figure 1: IRAS HIRES Serpens Core Images

FIG. 1.—*IRAS* HIRES Serpens core images: we present three panels for each *IRAS* waveband at 12, 25, 60, and 100 μm. The top panels show the single-iteration HIRES FRESCO images. The middle panels show in contours the results of differing levels of HIRES processing (lighter contours indicate fewer iterations). The bottom panels show our final adopted HIRES-processed "survey" images (*contours*) overlaid on the point-source "model" images (*gray scale*). All contours are separated by factors of 2 within the indicated ranges. At 12 μm: 1–16 MJy sr^{-1} (*top*), 5–640 MJy sr^{-1} (*middle and bottom*); at 25 μm: 1.5–24 MJy sr^{-1} (*top*), 10–640 MJy sr^{-1} (*middle and bottom*); at 60 μm: 20–320 MJy sr^{-1} (*top*), 50–3200 MJy sr^{-1} (*middle and bottom*); and at 100 μm: 80–320 MJy sr^{-1} (*top*), 100–6400 MJy sr^{-1} (*bottom*). The locations of the 12 point sources used to produce the "model" images described in the text are indicated by plus signs and crosses. Crosses distinguish sources that were inferred to be present based on matching the "model" images to the "survey" images.

TABLE 1

HIRES Point Sources in the Serpens Core

Source	Position[a] RA (1950)	DEC (1950)	Fluxes[b] 12 μm (Jy)	25 μm (Jy)	60 μm (Jy)	100 μm (Jy)	SED Properties T_{dust} (K)	$\tau_{250\mu m}$	L_{bol} ($L_\odot$)	Masses[c] M_c ($M_\odot$)	$M_c(H_2CO)$ ($M_\odot$)
FIRS1/SMM1	$18^h27^m17.5^s$	1° 13′ 15″	<0.6	5.6	170	435	27	0.1	46	3	0.25
SMM2	$18^h27^m28.0^s$	1° 10′ 45″	<0.6	<0.6	15	40	24	0.02	6	0.6	...
SMM3	$18^h27^m27.3^s$	1° 11′ 55″	<0.6	<0.6	22	70	24	0.03	8	0.9	2.9
SMM4	$18^h27^m24.7^s$	1° 11′ 10″	<0.6	<0.6	12	60	20	0.09	9	3	0.9
S68N	$18^h27^m15.5^s$	1° 14′ 50″	0.21[d]	1.5[d]	8[d]	37[d]	23	0.04	6	1.0	2.3
FU Ori	$18^h27^m16.8^s$	1° 14′ 15″	0.21[d]	1.5[d]	8[d]	37[d]	...	...	≤ 8	...	...
IRS53/SMM5	$18^h27^m18.9^s$	1° 14′ 36″	0.21[d]	1.5[d]	8[d]	37[d]	...	...	...	0.6	...
SVS20/SMM6	$18^h27^m25.4^s$	1° 12′ 02″	8.5	13	27	60	...	...	...	0.3	...
SVS2	$18^h27^m24.5^s$	1° 12′ 41″	2.5	5	27	75	...	...	...	...	...
SVS4	$18^h27^m26.0^s$	1° 10′ 50″	1.8	9.1	23	60	...	...	...	...	...
PS1	$18^h27^m27.1^s$	1° 09′ 54″	0.45	2	12	30	...	...	...	...	...
PS2	$18^h27^m30.4^s$	1° 10′ 24″	0.45	2	<6	< 12	...	...	...	...	...

[a]Positional references: FIRS 1, Curiel et al. 1993; FU Ori, Hodapp 1995; S68N, authors' unpublished H_2CO maps; SVS 2, Strom et al. 1976; SVS 4, PS 1, and PS 2, this paper; all others, Casali et al. 1993.

[b]Flux upper limits represent 3 σ detection limits for an unconfused point source.

[c]H_2CO masses are taken from Hurt et al. 1996 and represent warm gas emission only. For FIRS 1, where both warm and cold H_2CO emitting gas measurements are available, the *total* inferred gas mass is 3 $M_\odot$.

[d]This flux represents 1/3 of the total available flux from the region encompassing the three confused sources: S68N, FU Ori, and IRS 53/SMM 5. To be conservative, we used twice these flux values for the S68N SED fit.

extended on scales of 10″–20″ and/or embedded in a localized, diffuse component. Indeed, confusion from emission originating in the brightest NIR cluster region, SVS 4, is evident at 12 and 25 μm, and may, to a lesser extent, be a factor at 60 and 100 μm. We estimate that fluxes assigned to the "model" point sources can fluctuate by as much as ~20%, without significantly altering the map morphology. Combined with the 20% absolute uncertainty associated with HIRES fluxes (Levine & Surace 1993), we adopt overall uncertainties for our fluxes of 30%. If we allow for the presence of additional, relatively weak unresolved sources and for some contribution from an extended, diffuse component, the point-source fluxes we list in Table 1 are, strictly speaking, upper limits. For purposes of fitting source SEDs, we treated the listed flux upper limits for these objects as if they were the measured values.

3. RESULTS AND DISCUSSION

Figure 2 (Plate L5) shows the 25 μm HIRES-processed *IRAS* image of the Serpens core (*contours*) overlaid on the 1.1 mm continuum map (gray scale) of Casali et al. (1993), obtained with a 19″ beam. The locations and identifications of the 12 point sources we used to model the *IRAS* HIRES emission are also indicated. We identify two new *IRAS* point sources labeled PS1 and PS2 in Figure 2. PS1 has no clear NIR counterpart but is within 15″ (1 pixel) of a 1.3 mm continuum peak in a new, sensitive bolometer array map of the region at 12″ spatial resolution (André 1995). PS2 may be associated with the NIR source EC 129 ($K = 10$ mag; Eiroa & Casali 1992). None of the five previously proposed protostellar candidates of Hurt et al. (1996) are found to contribute at 12 μm, as expected for class 0 protostars (as noted in § 2, the flux attributed to S68N is an upper limit resulting from confusion, not a detection).

We combined published millimeter and submillimeter continuum fluxes (Casali et al. 1993; McMullin et al. 1994) with the fluxes and flux upper limits as listed in Table 1 to produce the SEDs for the Serpens sources. We then fitted the SEDs with modified blackbodies of the form

$$S_\lambda = B_\lambda(T_d)(1 - e^{-\tau_\lambda})d\Omega, \quad (1)$$

where $B_\lambda(T_d)$ is the standard Planck function, $d\Omega$ is the source size, and the dust optical depth τ_λ scales as $\lambda^{-1.5}$. We assumed 10″ source radii for all sources except FIRS 1, for which we adopted a 6″ radius (McMullin et al. 1994). From these fits, we determined the dust temperatures, T_d, and the dust optical depths, $\tau_{250\,\mu m}$, which are listed in Table 1. The SEDs of FIRS 1, SMM 2, SMM 3, and SMM 4 could be well fitted by single-component modified blackbodies with $T_d \leq 30$ K, a defining characteristic of class 0 protostars. Bolometric luminosities, L_{bol}, for these sources are obtained by integrating under the SED fits. In contrast, the SEDs of SVS 20/SMM 6, PS 1, and PS 2 could not be fitted by a single-component blackbody due to significant 12–25 μm excesses.

The SEDs of the three northernmost sources must be considered individually because of the confusion of fluxes. Adopting twice their tabulated fluxes as nominal upper limits, none are clearly fitted by a single blackbody component due to potential 12–25 μm excesses. This is certainly a valid assessment of IRS 53/SMM 5, which has significant 2.2 μm luminosity. The case is less clear for the recently discovered "FU Ori" source; we nonetheless place an upper limit of $L_{bol} < 8\,L_\odot$ on its preoutburst luminosity by integrating under its best-fit single-component SED and adjusting for the 12–25 μm excess. It is difficult to determine whether S68N actually possesses any 12–25 μm excess. Its significant millimeter flux and dense molecular core (Hurt et al. 1996) argue for a source in an early stage of evolution that is probably associated with the bulk of the 60–100 μm emission seen here. We tentatively adopt the best single-component blackbody fit (neglecting contributions at shorter wavelengths) for the temperature and luminosity of S68N and go on to show that its other properties are also consistent with class 0 sources.

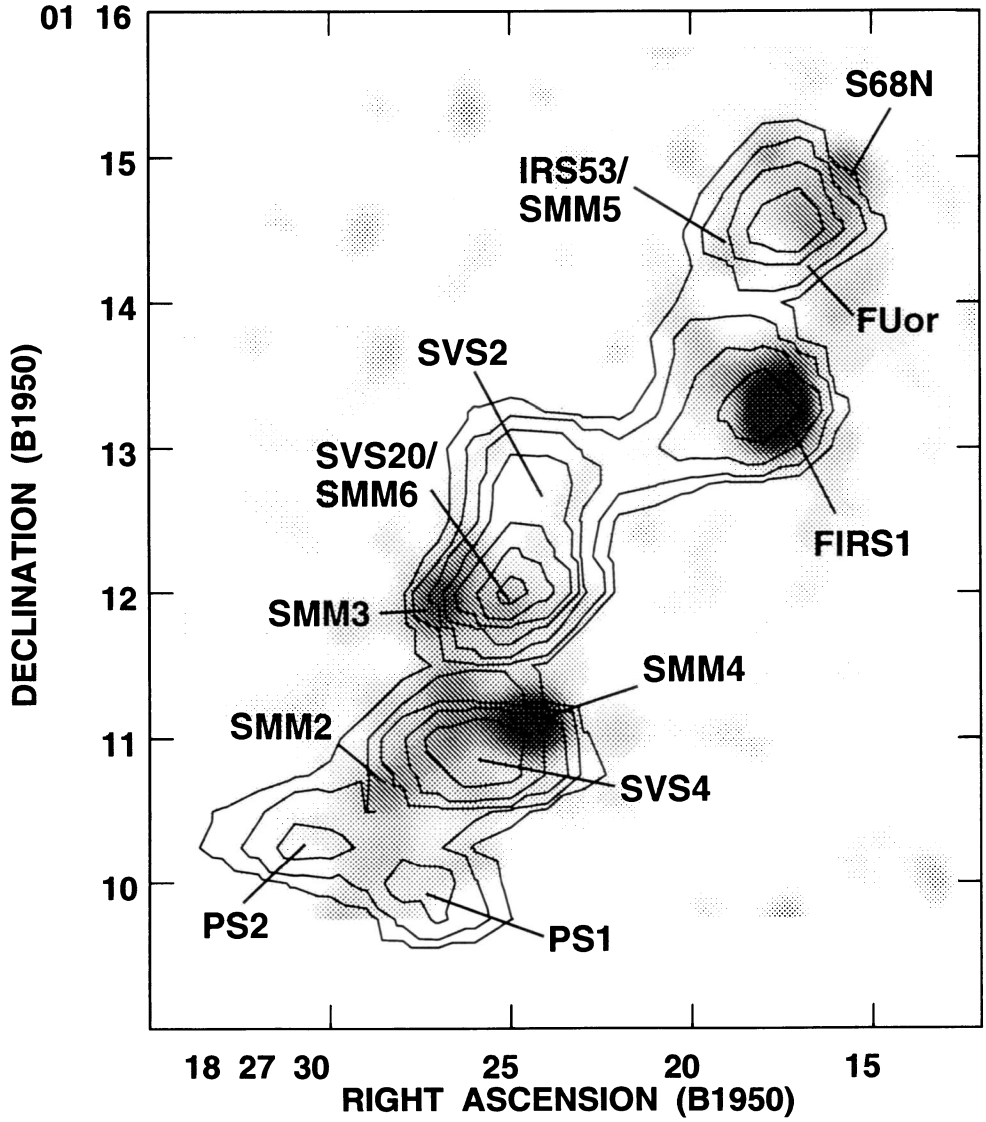

FIG. 2.—Comparison of the 25 μm and 1.1 mm emissions from the Serpens core: the HIRES-processed 25 μm emission (*contours*) is overlaid on the 1.1 mm continuum map (*gray scale*) of Casali et al. (1993). The 12 point sources used to model the region are all indicated and labeled. Note the offsets of the peaks of 25 μm emission from the millimeter peaks, indicating the relatively weak (and confused) 25 μm emission emanating from the class 0 sources.

HURT & BARSONY (see 460, L47)

Another indicator of class 0 status is the ratio of $L_{\rm bol}/(10^3 L_{1.3\,\rm mm})$. This ratio has values between 2 and 15 for class 0 objects, and values from 30 to 200 for class I objects (André et al. 1993). The values of this ratio are ~4 for SMM 4, ~7 for S68N, ~10 for SMM 2 and SMM 3, and ~12 for FIRS 1. Clearly, the Serpens sources fitted by a single-component blackbody curve satisfy this criterion for class 0 status.

We estimated circumstellar masses using the formula

$$M_c = \frac{S_\lambda d^2}{\kappa_\lambda B_\lambda(T_d)} \qquad (2)$$

(Hildebrand 1983), with $\kappa_{1.3\ \rm mm} = 0.01\ \rm cm^2\ g^{-1}$ at $\lambda = 1.3$ mm (André 1994). Circumstellar masses are also estimated for IRS 53 and SVS 20 using a single-component blackbody fit to the 60 μm–1.3 mm fluxes. The resultant circumstellar masses are listed in Table 1, along with previously determined circumstellar masses of the warm and cool gas components deduced from H_2CO measurements with the same assumed source sizes (Hurt et al. 1996). Granted the significant differences between these two methods of mass determination, the results agree quite well (within factors of 2–4). We note that the dust masses derived from the SEDs are insensitive to large changes (factors of 2 or more) in the assumed source size.

One final criterion for class 0 status is the presence of outflow activity. FIRS 1 is a famous outflow source (Curiel et al. 1993; Torrelles et al. 1992), SMM 4 has a recently discovered CO outflow (White, Casali, & Eiroa 1995), and S68N powers a water maser, which is always a sign of outflow activity in low-mass protostars (Wootten 1995). Current single-dish molecular line maps of the SMM 2 and SMM 3 regions have insufficient spatial resolution to distinguish any molecular outflows that may be present. Mapping of these sources awaits millimeter-interferometer observations.

We conclude that the Serpens core sources FIRS 1, S68N, SMM 2, SMM 3, and SMM 4 satisfy the defining criteria for class 0 protostars. This makes the Serpens core the richest known collection of this youngest class of forming stars. We note that, if for reasons discussed in § 2 our 60 and 100 μm fluxes are overestimates, then the argument for these sources being class 0 protostars is only strengthened, since we would be overestimating their temperatures and bolometric luminosities but not their circumstellar masses. In light of the expected short lifetimes of these sources (a few times 10^4 yr), we do seem to be witnessing "a second, recent wave of star formation" in Serpens, as suggested by Casali et al. (1993). Ongoing millimeter interferometric and single-dish observations will improve our understanding of the gas properties and kinematics in these young cores. Likewise, pending *Infrared Space Observatory* (*ISO*) observations will better resolve these sources and define their SEDs, as well as help determine the postoutburst luminosity of the "FU Ori" object, for which we have determined a preoutburst luminosity of $L_{\rm bol} < 8\ L_\odot$.

We are grateful to Deborah Levine and to Susan Terebey for insightful suggestions on the HIRES processing and to the IPAC staff for prompt handling of our data processing requests. We thank Alwyn Wootten for useful discussions and Philippe André for making his results available before publication.

REFERENCES

André, P. 1994, in Proc. 13 Rencontres de Moriond, The Cold Universe, ed. T. Montmerle, C. J. Lada, F. Mirabel, & J. Tran Thanh Van, (Gif-sur-Yvette: Editions Frontières), in press
———. 1995, private communication
André, P., Ward-Thompson, D., & Barsony, M. 1993, ApJ, 406, 122
Aumann, H. H., Fowler, J. W., & Melnyk, M. 1990, AJ, 99, 1674
Barsony, M. 1994, in ASP Conf. Ser. 65, Clouds, Cores, and Low-Mass Stars, Proc. 4th Haystack Conf., ed. D. P. Clemens & R. Barvainis (San Francisco: ASP), 197
Casali, M. M., Eiroa, C., & Duncan, W. D. 1993, A&A, 275, 195
Curiel, S., Rodríguez, L. F., Moran, J. M., & Cantó, J. 1993, ApJ, 415, 191
de Lara, E., Chavarria-K., C., & López-Molina, G. 1991, A&A, 243, 139
Eiroa, C., & Casali, M. M. 1989, A&A, 223, L17
———. 1992, A&A, 262, 468
Fowler, J. W., & Aumann, H. H. 1994, in Science with High-Resolution Far-Infrared Data, ed. S. Terebey & J. Mazzarella (JPL Publication 94-5), 1
Harvey, P. M., Wilking, B. A., & Joy, M. 1984, ApJ, 278, 156
Hildebrand, R. H. 1983, QJRAS, 24, 267
Hodapp, K. W. 1995, IAU Circ., No. 6186
Hurt, R. L., Barsony, M., & Wootten, A. H. 1996, ApJ, 456, 686
Levine, D. M., & Surace, J. 1993, in IPAC User's Guide (5th ed.; Pasadena: IPAC)
McMullin, J. P., Mundy, L. G., Wilking, B. A., Hezel, T., & Blake, G. A. 1994, ApJ, 424, 222
Strom, S. E., Vrba, F. J., & Strom, K. M. 1976, AJ, 81, 638
Torrelles, J. M., Gómez, J. F., Curiel, S., Eiroa, C., Rodríguez, L. F., & Ho, P. T. P. 1992, ApJ, 384, L59
White, G. J., Casali, M. M., & Eiroa, C. 1995, A&A, in press
Wootten, A. H. 1995, in preparation
Zhang, C. Y., Laureijs, R. J., & Clark, F. O. 1988, A&A, 196, 236